Acta Cryst. (1997). B53, 762–766

Radial Distribution of Electron Density in Magnetite, Fe_3O_4

SATOSHI SASAKI

Materials and Structures Laboratory, Tokyo Institute of Technology, Nagatsuta 4259, Midori, Yokohama 226, Japan. E-mail: sasaki@n.cc.titech.ac.jp

(Received 12 December 1996; accepted 27 May 1997)

Abstract

Radial electron distributions and net atomic charges of magnetite Fe_3O_4 have been studied using single-crystal X-ray intensity data up to $\sin\theta/\lambda = 1.22\,\text{Å}^{-1}$. The number of electrons, $C(R)$, was calculated against the radius of an atomic sphere for each atom by the Fourier summation method from the observed crystal structure factors. The radial distribution function was then obtained by differentiating the $C(R)$ curve to derive an electron distribution radius, r_{ED}, which can give a clear separation between neighboring atoms. The effective atomic charges of Fe ions thus obtained are +1.93 (4) e (A site) and +1.47 (4) e (B site), with $r_{ED} = 1.13$ and 1.19 Å, respectively. Fe ions occupying the A site are more ionic than those at the B site. The charge difference between sites A and B is +0.46 e, which is comparable to an ideal difference of +0.5 e between Fe^{3+} and $[Fe^{2+}Fe^{3+}]$. It suggests the existence of valence fluctuation between Fe^{2+} and Fe^{3+} in the B site. Crystal data: Fe_3O_4, $M_r = 231.54$, cubic, $Fd\bar{3}m$, $a = 8.375\,(2)$ Å, $V = 587.4\,(4)$ Å^3, $Z = 8$, $D_x = 5.23\,\text{Mg m}^{-3}$, $\lambda(\text{Mo } K\alpha) = 0.7107$ Å, $\mu(\text{Mo } K\alpha) = 14.88\,\text{mm}^{-1}$, $F(000) = 880$, $T = 296$ K, final $R = 0.016$ $wR = 0.010$ for 78 reflections averaged out of 6049 within a hemisphere, with $F > 3\sigma(F)$; $u = 0.2555\,(2)$.

1. Introduction

The basic chemical formula of spinel is generally given as AB_2X_4 (A: tetrahedral site, B: octahedral site) and magnetite belongs to this category. The cation distribution of magnetite is described as an inverse-spinel type, $Fe^{3+}[Fe^{2+}Fe^{3+}]O_4$ in contrast to Mn_3O_4 and Co_3O_4 of a normal-spinel type. At temperatures above the Verwey transition ($T_v \simeq 123$ K) magnetite belongs to cubic $Fd\bar{3}m$. The high electronic conductivity suggests the properties of valence fluctuation and the continuous interchange of electrons between Fe^{2+} and Fe^{3+} at the B sites (Verwey & Haayman, 1941). It is known to make the Fe ions frozen as charge ordering occurs below T_v (Iizumi *et al.*, 1982).

The spinel structure is characterized by the u parameter corresponding to the atomic coordinates of an O atom (Nishikawa, 1915; Bragg, 1915). The first experimental value of magnetite was $u = 0.379$ from X-ray intensity determination (Claassen, 1926). The structural consideration with the above u value leads to the conclusion that the ferric ions occupy the tetrahedral A site and ferric and ferrous ions are distributed at random among the octahedral B site. The above u parameter is equivalently transformed to 0.254 when the origin is taken at the center of symmetry. The structure was refined to give $u = 0.2548\,(2)$ from neutron diffraction data (Hamilton, 1958) and to give $u = 0.2549\,(1)$ from X-ray diffraction data (Fleet, 1981). The inverse-spinel configuration was suggested by the fast electron-hopping hypothesis (Verwey & de Boer, 1936) and supported by Mössbauer spectra with a six-line hyperfine structure below T_v (Bauminger, Cohen, Marinov, Ofer & Segal, 1961; Ito, Ono & Ishikawa, 1963).

The Mössauer spectrum above T_v has two components, of which one is due to Fe^{3+} at the A site and the other is due to Fe^{2+} and Fe^{3+} at the B site. The latter component of the spectrum shows broadening of the electron exchange with the relaxation time of 1.1 (2) ns at 300 K (Hargrove & Kündig, 1970). A molecular polaron model has been proposed for stoichiometric magnetite from the observation of Huang scattering in neutron scattering experiments above T_v (Yamada, Mori, Noda & Iizumi, 1979). The model describes valence fluctuation in a dynamically coupled cluster, based on a local charge density distribution of four Fe sites and displacements of the neighboring O atoms with an assumption on the local charge neutrality. It is expected that fluctuations in atomic positions couple to the valence fluctuation in magnetite.

In this paper we try to confirm the hopping scheme of Fe^{2+} and Fe^{3+} ions at the B site by means of X-ray diffraction and to explain little by little the origin of valence fluctuation at the B site. As a step forward, the charge differences of Fe ions in the A and B sites are examined in the determination of atomic charges from integration of the electron density within a sphere of the *electron distribution radius* [EDR; r_{ED} (Sasaki, Fujino, Takéuchi & Sadanaga, 1980)].

Table 1. *Final atomic parameters of magnetite*

	Fe (*A* site)	Fe (*B* site)	O
Wyckoff notation	8(*a*)	16(*d*)	32(*e*)
$x(=y=z)$†	1/8	1/2	0.2555 (2)
$u_{11}(=u_{22}=u_{33})$	0.0065 (2)	0.0067 (2)	0.0084 (4)
$u_{12}(=u_{12}=u_{23})$	0	0.0002 (2)	−0.0003 (8)
B_{eq} (Å^2)	0.515 (2)	0.527 (1)	0.665 (3)
$m-M$	Fe^{2+}–Fe^{3+}	Fe^{2+}–Fe^{3+}	O^{2-}–O^{-}
p‡	−0.9 (2)	−0.4 (2)	−0.84 (9)

† Origin at center ($\bar{3}m$), at (1/8, 1/8, 1/8) from $\bar{4}3m$. ‡ Atomic charges calculated from the p values are unrealistically +3.9, +3.4 and −0.2 e for Fe (*A*), Fe (*B*) and O, respectively.

2. Experimental

Single crystals used for the present study were synthesized from Fe_3O_4 powders (99%) at 1300 K in an evacuated silica tube. A single crystal was ground into a sphere of 0.08 mm in diameter and used for the X-ray study. The measuring device for X-ray diffraction was a Rigaku AFC-5 four-circle diffractometer with a graphite (002) monochromator; Mo $K\alpha$ radiation, 40 kV, 25 mA. The cell dimension measured in the diffractometry is $a = 8.375(2)$ Å. Integrated intensity data were collected using the ω–2θ scan technique (scan speed = 2° min^{-1}; scan width in $\omega = 1.2 + \tan\theta$ in °) within the range $2\theta \le 120°$ $(\sin\theta/\lambda \le 1.22)$, $-20 \le h \le 20$, $-20 \le k \le 20$, $0 \le l \le 20$. The intensity variation of a standard reflection, $\bar{4}40$, was kept less than ±1.9% throughout the data collection. Lorentz, polarization and spherical absorption effects were corrected. The transmission factors range from 0.418 to 0.459.

After averaging 6049 reflections ($R_{int} = 0.038$), 78 unique reflections with $F > 3\sigma(F)$ were used for simultaneous refinements of a scale factor, an extinction parameter, valence-occupancy parameters, atomic coordinates and temperature factors. The function $\Sigma w_i(|F_o| - k|F_c|)^2$ was minimized with $w_i = 1/\sigma^2(F)$ by the full-matrix least-squares program *RADY* (Sasaki, 1987), where k is a scale factor. An isotropic extinction correction was applied following Becker & Coppens (1974). The minimum value of $(F_o/kF_c)^2$ was 0.948 for the 400 reflection. The extinction type II parameter refined led to the radius of the mean particle being 0.14 (1) μm. Atomic scattering factors for Fe^{2+}, Fe^{3+} and O^- were taken from the *International Tables for X-ray Crystallography* (1974, Vol. IV) and that for O^{2-} was from Tokonami (1965). Valence-occupancy parameters p were simultaneously refined in the form

$$f(s) = f_M(s) + pf_{m-M}(s) + f' + if'' \qquad (1)$$

without the constraint on charge neutrality, where $s = \sin\theta/\lambda$ and m and M represent different ionic states. This procedure was performed to minimize the difference between F_o and F_c rather than the charge estimation. It was needed only in the procedure with the termination correction when the number of electrons, $C(R)$, was calculated. Anomalous scattering factors f' and f'' were taken from *International Tables for X-ray Crystallography* (1974, Vol. IV). Final refinement gave $R = 0.016$ and $wR = 0.010$ (goodness of fit, $S = 1.55$) with the maximum $\Delta/\sigma = 0.0002$ for the scale factor. Minimum and maximum heights in difference-Fourier maps are −2.0 and 0.9 e Å^{-3}, respectively. Atomic coordinates and temperature factors are listed in Table 1.† Interatomic distances are: Fe—O = 1.893 (2), O—O = 3.091 (2) Å for the *A* sites, Fe—O = 2.049 (2), O—O (*shared*) = 2.831 (2) and O—O (*unshared*) = 2.962 (2) Å for the *B* sites.

3. Calculation of the electron density distribution

In this study the atomic charge is defined as the number of electrons belonging to a specific atom, which can be given by

$$C(R) = \int \rho(r)\,dV, \qquad (2)$$

where R is the radius of an atomic sphere and $\rho(r)$ is the electron density at a point r in a unit cell. Equation (2) is represented as

$$\begin{aligned} C(R) &= \int V^{-1}\{\Sigma\Sigma\Sigma F(hkl)\exp(-2\pi i\mathbf{s}\cdot\mathbf{r})\}\,dV \\ &= V^{-1}\{(4\pi/3)R^3F(000) + (2\pi^2)^{-1}\Sigma\Sigma\Sigma' s^{-3}F(hkl) \\ &\quad \times(\sin 2\pi sR - 2\pi sR\cos 2\pi sR)\exp(-2\pi i\mathbf{s}\cdot\mathbf{r})\} \\ &\quad + \Delta C(R), \end{aligned} \qquad (3)$$

where s is redefined as $s = |\mathbf{s}| = 2\sin\theta/\lambda$ and $F(hkl)$ is the observed crystal structure factors. $\Delta C(R)$ is the correction term for the termination effect of the Fourier series outside the observed region and calculated with the Romberg numerical integration. $C(R)$ calculations were made using the program *ENAC* coded by K. Fujino (Sasaki, Fujino, Takéuchi & Sadanaga, 1980). The upper limit of the numerical integration was up to 99.97% of the distribution and the conversation criterion, EPS, was 5×10^{-5}. The observed structure factors were obtained using a relative scale factor in the charge refinement with the valence parameters described in (1). The structure factors for unobserved reflections were replaced by calculated ones. In this study, the above calculation was made with a radius increment of 0.005 Å up to 2 Å.

Figure 1 shows $C(R)$ curves before and after the correction for the Fourier termination. Full lines correspond to the curves after the correction, while open circles represent $C(R)$ values without $\Delta C(R)$ in (3). It is noted that the curve before the correction vibrates along to that after the correction. The vibration

† A list of structure factors has been deposited with the IUCr (Reference: OH0053). Copies may be obtained through The Managing Editor, International Union of Crystallography, 5 Abbey Square, Chester CH1 2HU, England.

period of the termination error for the *A* site [Fig. 1(*a*)] is very close to that for the *B* site [Fig. 1(*b*)].

Furthermore, the radial distribution of the electron density in an e Å^{-1} unit was estimated to differentiate (2) with respect to *R*

$$U(R) = 4\pi R^2 \rho(R) = \mathrm{d}C(R)/\mathrm{d}R. \quad (4)$$

According to the polynomial approximation, the differential curve is given as

$$U(R) = \Sigma(j-1)a_j R^{j-2} \quad (j = 2, 3, \ldots, N), \quad (5)$$

where the coefficients were obtained by means of a mean-square method with linear least-squares calculations of a polynomial equation of

$$C(R) = \Sigma a_j R^{j-1} \quad (j = 1, 2, 3, \ldots, N). \quad (6)$$

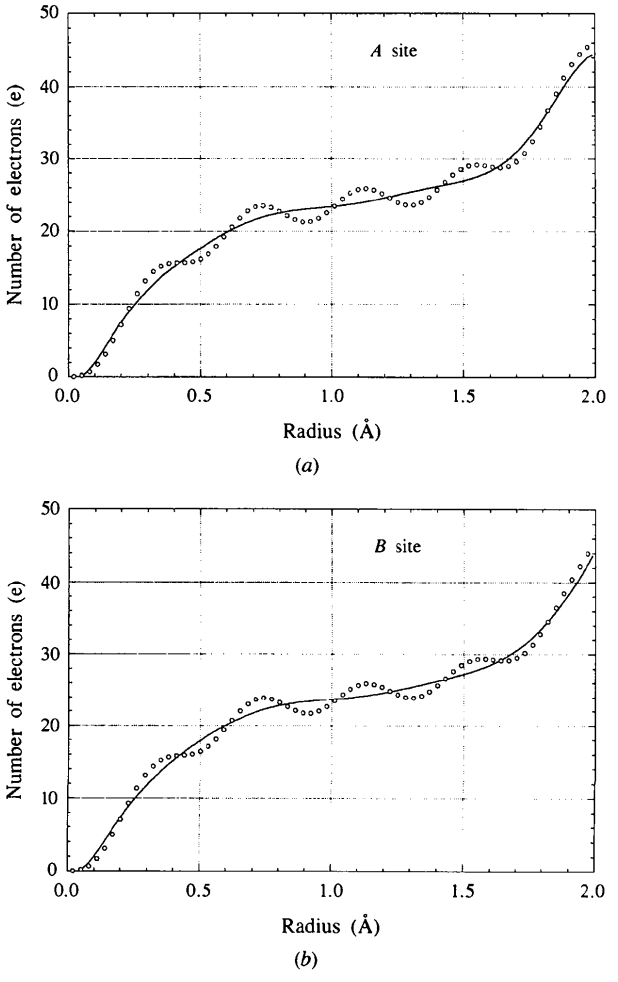

Fig. 1. The number of electrons *C*(*R*) *versus* radius *R*. (*a*) The Fe atom at the *A* site and (*b*) Fe atoms at the *B* sites in magnetite. Curves shown in solid lines and open circles represent after and before the termination correction, respectively.

Table 2. *List of R, C(R) and U(R) for Fe atoms at the A and B sites in magnetite*

Values in parentheses of *C*(*R*) represent the errors estimated from $\sigma F(hkl)$. The radii corresponding to various formal charges and r_{ED} are given in the 'Charge' column.

	Fe (*A* site)			Fe (*B* site)		
R (Å)	*C*(*R*) (e)	*U*(*R*) (e Å^{-1})	Charge	*C*(*R*) (e)	*U*(*R*) (e Å^{-1})	Charge
0.60	19.80 (2)	19.3		20.05 (2)	19.3	
0.64	20.53 (2)	17.2		20.78 (2)	17.1	
0.68	21.17 (2)	14.7		21.41 (2)	14.8	
0.72	21.71 (2)	12.2		21.96 (2)	12.4	
0.76	22.15 (3)	9.8		22.40 (2)	10.0	
0.80	22.49 (3)	7.5		22.76 (3)	7.9	
0.82	22.63 (3)	6.6		22.91 (3)	6.9	
0.84	22.75 (3)	5.7		23.04 (3)	6.0	+3
0.86	22.86 (3)	5.0		23.15 (3)	5.3	
0.88	22.95 (3)	4.4		23.25 (3)	4.6	
0.90	23.04 (3)	3.9	+3	23.34 (3)	4.0	
0.92	23.11 (3)	3.7		23.41 (3)	3.6	
0.94	23.18 (3)	3.5		23.48 (3)	3.3	
0.96	23.25 (3)	3.5		23.55 (3)	3.1	
0.98	23.32 (4)	3.6		23.61 (4)	3.0	
1.00	23.40 (4)	3.8		23.67 (4)	3.1	
1.02	23.48 (4)	4.1		23.73 (4)	3.2	
1.04	23.56 (4)	4.5		23.80 (4)	3.4	
1.06	23.66 (4)	5.0		23.87 (4)	3.7	
1.08	23.76 (4)	5.5		23.95 (4)	4.1	
1.10	23.88 (4)	6.0		24.03 (4)	4.5	+2
1.11	23.94 (4)	6.2		24.08 (4)	4.7	
1.12	24.00 (4)	6.5	+2	24.13 (4)	4.9	
1.13	24.07 (4)	6.7	r_{ED}	24.18 (4)	5.2	
1.14	24.13 (4)	6.9		24.23 (4)	5.4	
1.15	24.21 (4)	7.1		24.29 (4)	5.6	
1.16	24.28 (4)	7.3		24.34 (4)	5.9	
1.17	24.35 (4)	7.5		24.40 (4)	6.1	
1.18	24.43 (4)	7.7		24.47 (4)	6.3	
1.19	24.51 (4)	7.8		24.53 (4)	6.6	r_{ED}
1.20	24.58 (4)	8.0		24.60 (4)	6.8	
1.21	24.66 (4)	8.1		24.67 (4)	7.0	
1.22	24.75 (5)	8.1		24.74 (5)	7.2	
1.23	24.83 (5)	8.2		24.81 (5)	7.4	
1.24	24.91 (5)	8.2		24.88 (5)	7.6	
1.25	24.99 (5)	8.3	+1	24.96 (5)	7.7	
1.26	25.07 (5)	8.3		25.04 (5)	7.9	+1
1.27	25.16 (5)	8.2		25.12 (5)	8.0	
1.28	25.24 (5)	8.2		25.20 (5)	8.2	
1.29	25.32 (5)	8.1		25.28 (5)	8.3	
1.30	25.40 (5)	8.1		25.37 (5)	8.4	
1.32	25.56 (5)	7.9		25.54 (5)	8.6	
1.34	25.72 (5)	7.7		25.71 (5)	8.8	
1.36	25.87 (5)	7.5		25.89 (5)	9.0	
1.38	26.02 (5)	7.3	0	26.07 (5)	9.1	0
1.40	26.16 (5)	7.2		26.25 (5)	9.3	
1.42	26.30 (5)	7.2		26.44 (5)	9.4	
1.44	26.45 (5)	7.3		26.63 (5)	9.7	
1.46	26.60 (6)	7.7		26.83 (6)	9.9	
1.48	26.76 (6)	8.3		27.03 (6)	10.3	
1.50	26.93 (6)	9.1		27.24 (6)	10.8	
1.52	27.12 (6)	10.3		27.46 (6)	11.4	
1.54	27.34 (6)	11.8		27.70 (6)	12.2	
1.56	27.60 (6)	13.6		27.95 (6)	13.1	
1.58	27.89 (6)	15.9		28.22 (6)	14.2	
1.60	28.24 (6)	18.5		28.52 (6)	15.5	
1.64	29.10 (6)	24.8		29.21 (6)	18.8	
1.68	30.23 (6)	32.2		30.04 (6)	23.0	
1.72	31.68 (6)	40.2		31.05 (6)	27.9	

By using the program *POED*, the calculation with $N = 12$ in (6) was adopted for all atoms of magnetite with R factors 0.9, 0.8 and 1.0% for the A, B and oxygen sites, respectively. The use of the differential equation may have the effect that the small amount of uncorrected termination term is rounded, but the total fitness loses the fine structure. The $C(R)$ and $U(R)$ values are listed in Table 2 within the radius range from 0.60 to 1.72 Å for the A and B sites.

The $U(R)$ curves of Fe atoms for the A and B sites are shown in Fig. 2(*a*). In the $U(R)$ curve the first peak gives the electron distribution of the Fe atom, while the second peak near 2 Å is of the O atom, where the peak position mainly depends on the Fe—O interatomic distance. Within the first peak of $U(R)$, a sharp peak around $R \simeq 0.15$ Å corresponds to the distribution of core electrons of Fe and a hump on the peak shoulder around $R \simeq 0.6$ Å and its outer region correspond to that of $3d$ electrons of Fe. Such a characteristic of $U(R)$ resembles those previously reported (Sasaki, Fujino & Takéuchi, 1979; Fujino, Sasaki, Takéuchi & Sadanaga, 1981; Sasaki, Takéuchi, Fujino & Akimoto, 1982). The $U(R)$ curve of the O atom is shown in Fig. 2(*b*). It is known that small humps of $U(R)$ around $R \simeq 0.15$ and 0.45 Å are mainly due to $1s^2$ and $2s^2$ electrons, respectively.

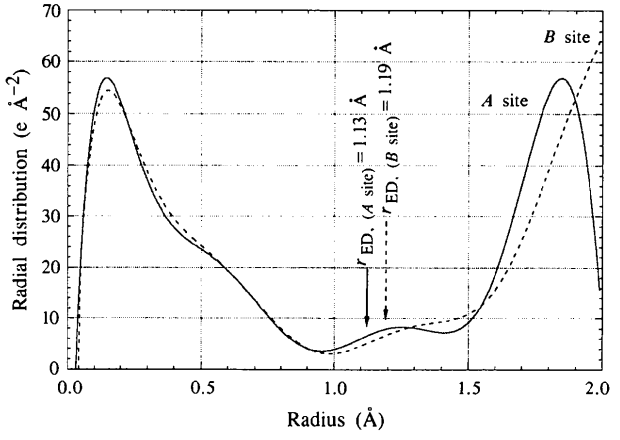

Fig. 2. Curves of $U(R)$ *versus* R for (*a*) the Fe atoms in the A site (solid line) and the B site (broken line) and (*b*) the O atoms. The radii r_{ED} determined for magnetite are plotted with arrows.

4. Results and discussion

The atomic radius r_{ED} and effective atomic charge are now estimated from the analysis of $C(R)$ and $U(R)$ curves. In the case where the $U(R)$ curve has a flat and low electron-density region between Fe and O atoms, the radius r_{ED} can be plausibly estimated from the change in $U(R)$ curvature so that the $U(R)/dR$ curve in Fig. 3 gives a unique solution (Sasaki, Fujino, Takéuchi & Sadanaga, 1980). Then, the electron distribution radius for the *flat* type is approximately given as

$$r_{ED} = (2R_m + R_o)/3, \quad (7)$$

where R_m and R_o are the points with the averaged gradient of the flat region of $U(R)$. Each point roughly describes an end of the shoulder of the $U(R)$ peak occupied by the electrons of the respective Fe and O atoms. As shown in Fig. 3, the related values are $R_A = 0.98$, $R_{O(A)} = 1.43$, $R_B = 1.05$ and $R_{O(B)} = 1.46$ Å, where $m = A$ or B; $O = O(A)$ or $O(B)$ for the A and B sites. Accordingly, $r_{ED} = 1.13$ (A site) and $r_{ED} = 1.20$ Å

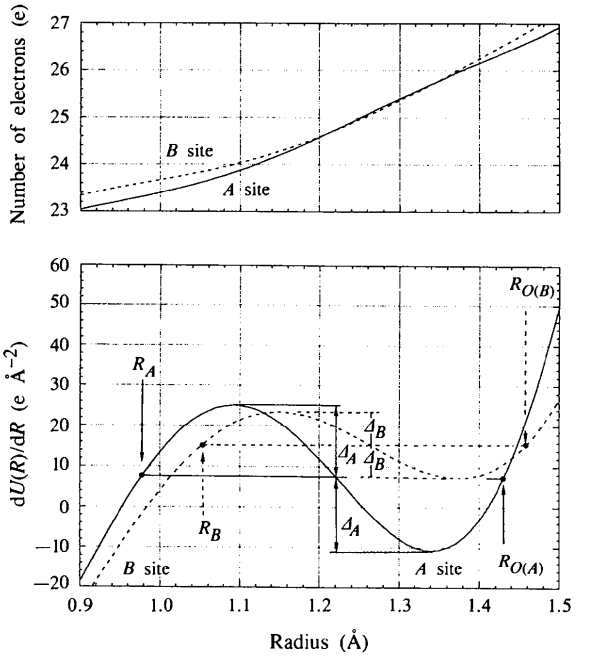

Fig. 3. Curve of $dU(R)/dR$ *versus* R for the Fe atoms in A and B sites, associated with $C(R)$. R_A, R_B, $R_{O(A)}$ and $R_{O(B)}$ are defined in the text; Δ_A and Δ_B indicate the midpoints between the maximal and minimal of $dU(R)/dR$ curves for the A and B sites, respectively.

(*B* site). It should be noted that the radius r_{ED} represents the electron distribution and is much longer than the ionic and crystal radii (Shannon & Prewitt, 1969): the ionic and crystal radii of Fe^{3+}(IV), Fe^{3+}(VI) and Fe^{2+}(VI) at the high-spin state are 0.49, 0.645 and 0.78 Å and 0.63, 0.785 and 0.92 Å, respectively.

The $C(R)$ values and atomic charges corresponding to the above r_{ED} are 24.07 (4) and +1.93 (4) e for the Fe atoms at the *A* site, while 24.53 (4) and +1.47 (4) e for those at the *B* sites. The charge difference between the *A* and *B* sites is 0.46 e and coincides very well with an ideal charge difference of 0.5 e between the two sites. The atomic charges obtained for magnetite are comparable with the values previously reported for iron silicates: +1.20 e (r_{ED} = 1.11 Å) for Fe_2SiO_4 (Fujino, Sasaki, Takéuchi & Sadanaga, 1981); +1.12 e (r_{ED} = 1.14 Å) for $Fe_2Si_2O_6$ (Sasaki, Takéuchi, Fujino & Akimoto, 1982).

In conclusion, Fe ions at the *A* site are more ionic than those at the *B* site. The charge difference is 0.46 e per atom, which is very close to 0.5 e, an ideal difference between Fe^{3+} and [$Fe^{2+}Fe^{3+}$]. Thus, the present study supports a commonly accepted concept on mixed-valence magnetite that Fe^{3+} ions selectively occupy the *A* site and Fe^{2+} and Fe^{3+} ions distribute in half among the *B* sites.

References

Bauminger, R., Cohen, S. G., Marinov, A., Ofer, S. & Segal, E. (1961). *Phys. Rev.* **122**, 1447–1450.

Becker, P. J. & Coppens, P. (1974). *Acta Cryst.* A**30**, 129–147.

Bragg, W. H. (1915). *Philos. Mag.* **30**, 305–315.

Claassen, A. A. (1926). *Proc. Phys. Soc.* **38**, 482–487.

Fleet, M. E. (1981). *Acta Cryst.* B**37**, 917–920.

Fujino, K., Sasaki, S., Takéuchi, Y. & Sadanaga, R. (1981). *Acta Cryst.* B**37**, 513–518.

Hamilton, W. C. (1958). *Phys. Rev.* **110**, 1050–1057.

Hargrove, R. S. & Kündig, W. (1970). *Solid State Commun.* **8**, 303–308.

Iizumi, M., Koetzle, T. F., Shirane, G., Chikazumi, S., Matsui, M. & Todo, S. (1982). *Acta Cryst.* B**38**, 2121–2133.

Ito, A., Ono, K. & Ishikawa, Y. (1963). *J. Phys. Soc. Jpn*, **18**, 1465–1473.

Nishikawa, S. (1915). *Proc. Tokyo Math. Phys. Soc.* **8**, 199–209.

Sasaki, S. (1987). *RADY*. KEK Internal Report 87-3. National Laboratory for High Energy Physics, Japan.

Sasaki, S., Fujino, K. & Takéuchi, Y. (1979). *Proc. Jpn. Acad. B*, **55**, 43–48.

Sasaki, S., Fujino, K., Takéuchi, Y. & Sadanaga, R. (1980). *Acta Cryst.* A**36**, 904–915.

Sasaki, S., Takéuchi, Y., Fujino, K. & Akimoto, S. (1982). *Z. Kristallogr.* **158**, 279–297.

Shannon, R. D. & Prewitt, C. T. (1969). *Acta Cryst.* B**25**, 925–946.

Tokonami, M. (1965). *Acta Cryst.* **19**, 486.

Verwey, E. J. W. & de Boer, J. H. (1936). *Rec. Trav. Chim. Pays-Bas*, **55**, 531–540.

Verwey, E. J. W. & Haayman, P. W. (1941). *Physica*, **8**, 979–987.

Yamada, Y., Mori, M., Noda, Y. & Iizumi, M. (1979). *Solid State Commun.* **32**, 827–830.